Molecular-dynamic calculation of the relaxation of the electron energy distribution function in a plasma

N. David and S. M. Hooker
Department of Physics, University of Oxford, Clarendon Laboratory, Parks Road, Oxford OX1 3PU, United Kingdom
(Received 28 July 2003; published 3 November 2003)

A molecular-dynamic (MD) code is used to calculate the temporal evolution of nonequilibrium electron distribution functions in plasmas. To the authors' knowledge, this is the first time that a molecular-dynamic code has been used to treat this problem using a macroscopic number of particles. The code belongs to the class of P^3M (particle-particle-particle-mesh) codes. Since the equations solved by the MD code are fundamental, this approach avoids several assumptions that are inherent to alternative methods. For example, the initial energy distribution can be arbitrary, and there is no need to assume a value for the Coulomb logarithm. The advantages of the MD code are illustrated by comparing its results with those of Monte Carlo and Fokker-Planck codes with a set of plasma parameters for which the Fokker-Planck calculation is shown to give incorrect results. As an example, we calculate the relaxation of the electron energy distribution produced by optical field ionization of a mixed plasma containing argon and hydrogen.

DOI: 10.1103/PhysRevE.68.056401 PACS number(s): 52.65.Yy, 52.65.Ff, 52.65.Pp, 42.55.Vc

I. INTRODUCTION

The general question of how a given distribution of electron velocities in a plasma reaches equilibrium has been of interest for some time; the first calculations being those undertaken by Spitzer [1] and Dolinsky [2] more than 40 years ago. The time taken for the electron energy distribution to reach equilibrium is often very short compared to time scales of interest, in which case it is appropriate to treat the electrons as being in local equilibrium with a well-defined temperature. However, following the development of short-pulse laser systems, knowledge of the formation and evolution of the electron energy distribution on picosecond and femtosecond time scales is important in a wide range of applications. In the light of this Spitzer and Dolinsky's results have been incorporated in a number of modern numerical computer codes [3,4]. Most codes solve the Fokker-Planck equation, i.e., the Vlasov equation for the evolution of the velocity distribution of charged particles with an additional collision term. In most cases, as in this paper, the particles are treated nonrelativistically.

The reason one has to use the Fokker-Planck equation, instead of using a two-body collision calculation, is the long-range effect of the Coulomb field. So, instead of making predominantly short-range, two-body collisions, the electrons are constantly subject to weakly scattering, many-particle collisions. In the Fokker-Planck equation the collision term is derived from the two-particle scattering cross section. However, since the cross section diverges for large impact parameters, one normally introduces a long-range cutoff b_{max} for the impact parameter. This cutoff is generally related to the Debye length of a plasma $\lambda_{Debye}=\sqrt{\epsilon_0 T/e^2 n_e}$ in which T is the electron temperature in Joules and n_e is the electron density. Using this long-range cutoff and a further cutoff b_{min} for short-range, large angle collisions, which is related to the de Broglie wavelength $\lambda_{deBroglie}=h/\sqrt{3mT}$ and the classical distance of closest approach e^2/mv^2, one can define the Coulomb logarithm $\ln\Lambda$. The Coulomb logarithm is an important parameter of the collision term, and there exist a number of different definitions of this quantity, depending on the plasma conditions, but it is essentially of the form $\ln\Lambda=\ln(b_{max}/b_{min})$ [5,6].

The approximations inherent in the use of the Coulomb logarithm may be illustrated as follows. For a plasma with $n_e=10^{19}$ cm^{-3} and $T=4$ eV the Debye length is $\lambda_{Debye}=4.7$ nm. In this case the number of particles contained in the Debye sphere $N_{Debye}=\frac{4}{3}\pi\lambda_{Debye}^3 n_e\approx 5$. Since this is not a large number, shielding of charge fluctuations on the scale of the Debye length will not be complete and hence the use the Debye length as the long-range limit in the Coulomb logarithm is likely to lead to errors. We note that the requirement for the Debye shielding picture to be correct, $N_{Debye}\gg 1$, is equivalent to $\Gamma=e^2/(\epsilon_0\lambda_{Debye}T)\ll 1$, where Γ is the plasma coupling parameter. Consequently the Spitzer formulas are only valid for weakly coupled plasmas. In addition to the general problem of the Coulomb logarithm, the Spitzer calculations require a velocity distribution that is close to equilibrium to be valid. This means that a large proportion of the particles have to be in a Maxwell-Boltzmann distribution and the speed of the ''test'' particles whose equilibration is being calculated must not be considerably larger than the thermal speed of the background plasma.

The molecular-dynamic (MD) approach employed here has the advantage of being derived from a more fundamental set of equations, with fewer assumptions. One does not need to define a Coulomb logarithm; instead all that is needed for the nonrelativistic calculation are the electrostatic Maxwell equations and Newton's equations of motion. Consequently, MD calculations can be employed for plasma conditions under which alternative approaches lead to significant errors, as well as providing a reliable test for faster approximations. The major disadvantage of this method is its speed. Since every particle has to be treated individually, and a rather large number of particles is needed to reach statistically meaningful results, MD codes are slow compared to other approaches. It is therefore of particular importance to use

algorithms where the number of steps is a low-order function of the number of particles.

Molecular-dynamic calculations of the temperature relaxation of a strongly coupled two-temperature plasma were first performed by Hansen and McDonald [7] in 1983 and later by Reimann and Toepffer [8] in 1990. In these early papers the equations of motion for a small number of charged particles were integrated directly. Owing to the small number of particles used (128 and 108, respectively), it was not possible to investigate the behavior of an energy distribution function. Instead, only statements on the mean energy of two particle groups with well-defined initial temperatures could be made. The calculated relaxation times agreed surprisingly well with the Spitzer values even though coupling parameters of up to $\Gamma=5$ were being simulated. In a somewhat different context, Murillo [9] has employed a MD code to investigate the possibility of forming a strongly coupled ion plasma from a cold atomic gas. Furthermore, Zwicknagel *et al.* [10] used a MD code to calculate results concerning the stopping power of heavy ions by electrons.

In this paper we describe what is to our knowledge the first molecular-dynamic code for calculation of the relaxation of an arbitrary electron energy distribution in a plasma. In Sec. II we outline the operation of the code. In Sec. III A we compare its results against several test cases for plasma conditions under which alternative methods are valid. In Sec. III B we discuss in detail a case for which the Fokker-Planck method gives inaccurate results, and we compare the results of those codes with those from Monte Carlo and MD codes. In Sec. III C we consider an example case which is of current interest in the study of new types of short-wavelength laser, and in Sec. IV we conclude.

The calculations were performed on a 2.4-GHz personal computer and took 3 days on average for a calculation of the evolution of the energy distribution of 2×10^5 particles over 10 ps.

II. THE MOLECUAR-DYNAMIC CALCULATION

A. The P^3M Method

Solving the individual force equations for each of the N particles in a system would require $N^2/2$ individual force calculations to be undertaken every integration time step. In addition, the time step would have to be small enough to resolve even the hardest collisions. In total, this method would end up taking several years for a simple calculation with 2×10^5 particles, even if the conservation errors that inevitably accompany integration over many time steps were neglected. A large reduction in the number of calculations required can be achieved by employing the particle-particle-particle-mesh (P^3M) method first described by Hockney and Eastwood [11]. In this method the force on a particle is divided into a collective, long-range term from the majority of the particles (particle-mesh); and a short-range, strong-force term by the particles close to the particle in question (particle-particle). Using this general idea, we chose to calculate the long-range effects by solving the Poisson equation on a mesh, and treating the short-range effects by using the analytical two-body solution for an electron-electron collision. The P^3M method has recently been used by Donko *et al.* [12] for molecular-dynamic studies of strongly coupled charged particle bilayers. The problem considered was therefore a two-dimensional (2D) one. In that work the short-range collisions were calculated using a Coulomb correction term, not by employing the analytical trajectories.

In our code the coordinate space is a 3D cube, represented by a 64^3-point grid. The boundary conditions are chosen to be periodic. The long-range effects are then treated by solving the Poisson equation on the mesh with a fast Fourier transform (FFT) [13]. To ensure that collisions are not treated twice, particles are treated as if they were positioned at the closest grid point since particles that are at the same grid point do not feel each other [14,15]. Solution of the Poisson equation and the evolution of the electron velocity distribution in the associated electric field is achieved by a set of difference equations in the usual way [16,17]. Note that the ions are treated as a positive background, because the energy exchange between them and the electrons is very slow as a result of the large difference in mass.

The system of differential equations is

$$\Delta\Phi(\vec{x})=-\frac{\rho(\vec{x})}{\epsilon_0}, \tag{1}$$

$$\vec{E}(\vec{x})=-\vec{\nabla}\Phi, \tag{2}$$

$$m\frac{d\vec{v}}{dt}=q\vec{E}(\vec{x}), \tag{3}$$

where m is the electron mass, q is the electron charge, Φ is the electrostatic potential, $\vec{E}$ is the electric field, and ρ is the charge density.

Introducing the distance x_0, which defines the length of a single side of a cell, one can define dimensionless space, time, density, and electric fields:

$$\vec{x}'=\frac{\vec{x}}{x_0}, \tag{4}$$

$$t'=\frac{ct}{x_0}, \tag{5}$$

$$\rho'=\rho\frac{x_0^3}{e}, \tag{6}$$

$$\Phi'=\frac{x_0\epsilon_0}{e}\Phi, \tag{7}$$

$$\vec{E}'=\frac{\epsilon_0 x_0^2}{e}\vec{E}. \tag{8}$$

Defining the dimensionless parameter $\alpha=e^2/\epsilon_0 c^2 x_0 m$, and dropping the primes, our set of equations becomes

$$\Delta\Phi(\vec{x})=-\rho, \tag{9}$$

$$\vec{E}(\vec{x}) = -\vec{\nabla}\Phi, \tag{10}$$

$$\frac{d\vec{v}}{dt} = \alpha\vec{E}(\vec{x}). \tag{11}$$

Equation (9) is then solved using two FFTs [13]. The calculation time for a FFT is proportional to $N_{\text{cell}}\ln N_{\text{cell}}$, where N_{cell} is the number of cells. Provided that the number of cells is not much larger than the number of particles N, the time to calculate the FFT is very much shorter than that required to solve the $N^2/2$ force equations.

B. Energy renormalization

A known problem with solving the field equations on a mesh and then using a difference equation to accelerate particles is that energy is not conserved. While this effect is very small, it leads to an overall increase in electron energy after many time steps and, given that we are interested in determining the evolution of the electron energy distribution, this effect must be canceled by regular renormalization. In order for the renormalization to not change the physics one is trying to observe, the renormalization has to have the same velocity dependence as the erroneous energy gain.

Since the problem is treated nonrelativistically, the forces, and hence the momentum transfer, are independent of velocity. If a particle with momentum $\vec{p}$ is erroneously given an additional, unphysical momentum $\vec{\Pi}$, the resulting error in the energy of the particle is

$$\delta E = \frac{1}{2m}[(\vec{p}+\vec{\Pi})^2 - \vec{p}^2] = \frac{\vec{p}\cdot\vec{\Pi}}{m} + \frac{\Pi^2}{2m}.$$

For an isotropic momentum distribution the term $\vec{p}\cdot\vec{\Pi}/m$ will average to zero, and hence the average energy error per particle will be $\overline{\delta E} = \overline{\Pi}^2/2m$. Since the total energy of the system is known to be constant, the total energy error δE_{tot} can be calculated easily. For N particles this results in an average error per particle $\overline{\delta E} = \delta E_{\text{tot}}/N = \overline{\Pi}^2/2m$.

The average energy error $\overline{\delta E} = \overline{\Pi}^2/2m$ may be written as

$$\frac{\overline{\Pi}^2}{2m} = \frac{\overline{\Pi}_x^2 + \overline{\Pi}_y^2 + \overline{\Pi}_z^2}{2m} = \frac{\overline{\Pi}_\parallel^2 + \overline{\Pi}_\perp^2}{2m},$$

where $\overline{\Pi}_\parallel^2$ is the average energy gain due to unphysical momentum displacements parallel to the velocity vector of the electron, and $\overline{\Pi}_\perp^2$ is the energy gain due to displacements perpendicular to the velocity of the electron. Using simple 3D symmetry relations for an isotropic distribution yields

$$\overline{\Pi}_\perp^2 = 2\overline{\Pi}_\parallel^2 = \frac{2\overline{\Pi}^2}{3}. \tag{12}$$

For a single particle with true momentum $\vec{p}$ the displaced momentum is $\vec{p}_d = \vec{p} + \vec{\Pi}_\parallel + \vec{\Pi}_\perp$. This results in an erroneous energy gain $\delta E = (\vec{\Pi}_\parallel^2 + \vec{\Pi}_\perp^2 + 2\vec{p}\cdot\vec{\Pi}_\parallel)/2m$. Since the average value of $\vec{p}\cdot\vec{\Pi}_\parallel$ is zero, from this last result we recover $\overline{\delta E} = (\overline{\Pi}_\perp^2 + \overline{\Pi}_\parallel^2)/2m = \overline{\Pi}^2/2m$. However, the term $\vec{p}\cdot\vec{\Pi}_\parallel$ is important since it can change the shape of the velocity distribution function. Since one does not know the sign of this product for any individual particle, statistical properties have to be used. For a particle with displaced total momentum $|\vec{p}_d|$ the probability that its true momentum is $|\vec{p}_d| - |\overline{\Pi}_\parallel|$ is proportional to the value of the distribution function for this momentum. Similarly the probability for the particle to have a true momentum of $|\vec{p}_d| + |\vec{\Pi}_\parallel|$ is proportional to the respective value of the distribution function. Therefore in each time step, and for each particle, a Monte Carlo procedure is used to determine whether the particle is moved to higher or lower momentum. In so doing the energy correction $(\Pi_\parallel^2 + \vec{p}\cdot\vec{\Pi}_\parallel)/2m$ has been accounted for. It only remains to subtract the term $\overline{\Pi}_\perp^2/2m$ from the energy of each particle.

C. Analytical two-body collision

Collisions between particles inside the same cell are treated explicitly using the analytical two-body solution. For each time step and for each cell the program determines how many particles are in the cell. Whenever there is more than one particle in a cell it treats all collisions as two particle analytical collisions in the respective center of mass frame. In general these frames will be weakly accelerated frames due to the effect of the global electric field. The known analytical hyperbolic solution [18] is used to determine the exact momentum transfer the two particles experience in passing through the whole cell. Since it can take slow particles as many as 30 time steps to pass a single cell, the momentum transfer is always done at the time step during which the particles pass each other. If there are only two particles in the cell, this yields the correct momentum transfer. We chose to calculate the momentum transfer for a cell passage instead of for each time step, since the latter would result in a momentum transfer error due to the finite time step especially for fast particles. These particles could have traveled nearly halfway across the cell the first time they enter it. By calculating the momentum transfer for a cell passage we minimize errors in the momentum transfer. Of course, this approach can lead to small errors in the calculated positions of the two particles. However, we are interested in the velocity distribution and not in the exact positions of the particles.

Figure 1 illustrates how the two-particle scattering is treated. The positions of the particles at the previous time step are illustrated by open circles. If during the next time step it is calculated that the particles would pass each other, the particles are given their initial momenta for half the time step and the final momenta of the analytic solution for the remaining half. In this way the full analytical curve (dashed) is approximated by straight sections.

The momentum transfer calculation is performed in the center of mass frame, so that the two-particle problem can be converted into a one-particle problem. In this mathematical frame, the other quantities needed to calculate the momentum transfer are the angular momentum l, the relative velocity v_{rel} and the total energy of the relative motion $E = \frac{1}{2}\mu\dot{r}^2 + l^2/(2\mu r^2) + \alpha'/r$, where μ is the reduced mass

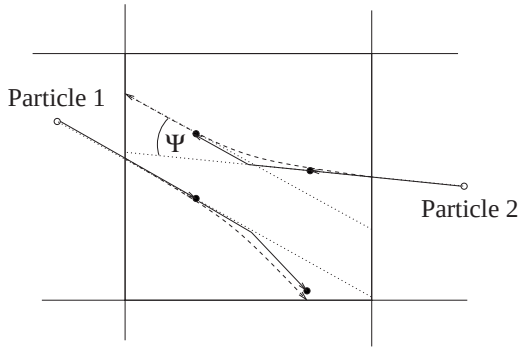

FIG. 1. Schematic diagram showing how scattering of two electrons within a single cell is treated.

and $\alpha' = \alpha/4\pi$. The total scattering angle Ψ' (in the center of mass frame) for the particle traveling across the whole cell can then be calculated:

$$\cos\left(\frac{\Psi'}{2}\right) = \frac{4lE/\alpha' - 2l/r}{v_{rel}\sqrt{1+4l^2E/\alpha'^2}}, \tag{13}$$

where $\mu = 0.5$ has already been substituted

The parameter r appearing in the numerator is the distance the two particles are apart at the beginning of the calculation. Since the resolution of the discrete mesh is 1, we set $r = 1$. Clearly this is an approximation. However, we note that setting r equal to the particle separation at the beginning of the time step is incorrect since the particles would have interacted from the moment they both entered the same cell. It would also be incorrect to set r equal to the distance between the two points where the particle trajectories cross the boundary of the cell, since in reality they would also have interacted when they were outside the cell. Within the MD approach interaction between particles in different cells is treated in an average way through the Poisson equation which will tend to underestimate the force between particles entering the same cell. Hence taking $r = 1$ for all collisions is a sensible compromise.

There are a number of problems with this approach that should be acknowledged. With a finite time step, two particles on the border of adjacent cells might swap cells without feeling the hard analytical repulsion. This problem can always be reduced by a smaller time step, but never eliminated. There is therefore a small percentage of hard encounters not taken into account. For the parameters used in the calculations presented in this paper, approximately 1% of hard two-body encounters are lost.

A second problem arises when there are three particles in a cell since they are treated as three two-body collisions instead of one three-body collision. In most cases this will not make a significant difference. Even though the number of cells used is larger then the particle number, there is still a certain fraction of cells that hold three or more particles. For 64^3 cells and 2×10^5 particles there are of the order of 10^4 cells, i.e., ≈4%, that contain three or more particles. However, the cross section for three-particle collisions is usually rather small. For example, for a typical collision between a fast and a slow particle of total energy 50 eV to result in a significant momentum transfer, i.e., one that would yield a scattering angle of $\Psi' > 0.5$ rad, the impact parameter b would have to be $b < 0.024$ [Eq. (13)]. This corresponds to a cross section $\sigma_2 = \pi b^2 \approx 0.0018$. If this is multiplied by the average distance that the fast particle covers in one time step, this would result in a volume $V_{coll} \approx 1.8\times10^{-4}$. A three-body collision with significant momentum transfer will occur if there are two other particles within this volume. The probability for this to occur is $P_3 \approx (V_{coll}^2) \approx 3\times10^{-8}$. If this probability is multiplied by the number of cells with three or more particles, it gives an estimate as to how often a significant three-body-collision occurs. This is roughly every $t_3 = (10^4 P_3)^{-1} \approx 3000$ time steps. Considering the large number of collisions every time step, this small proportion can safely be neglected.

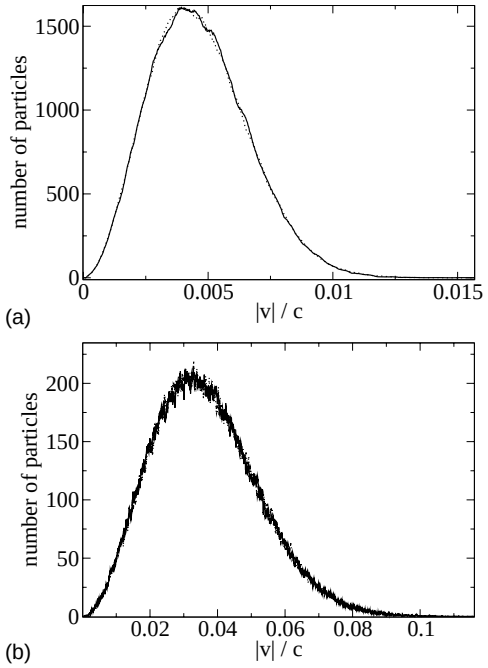

FIG. 2. Calculated evolution of Maxwell-Boltzmann speed distributions for initial temperatures of (a) 4 eV, (b) 245 eV. For both calculations the electron density was 10^{19} cm^{-3}; the initial distribution is shown by the dotted curve, and the distribution after 10 ps by the solid line.

III. RESULTS

A. Tests

We have tested the code described above against several calculations by earlier authors. Before describing these, we note that if the initial electron energy distribution is a Maxwellian distribution over velocities, the calculated distribution should not change shape apart from the statistical fluctuations that are always present when working with a finite number of particles. Figure 2 shows the calculated evolution of Maxwell-Boltzmann speed distributions for initial temperatures of (a) 4 eV and (b) 245 eV. For both calculations the initial distribution is compared with that calculated after

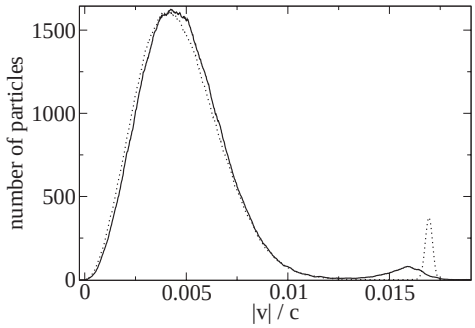

FIG. 3. Calculated evolution of a two-temperature electron energy distribution with $T_f=4$ eV and $T=54.4$ eV. The initial distribution is shown by a dotted line and the calculated distribution after 10 ps by a solid line.

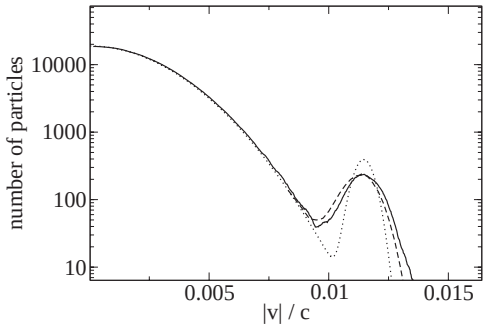

FIG. 4. Comparison of the results of the MD calculation (solid line) with the results of Dolinsky (dashed line) for relaxation of a Maxwell-Boltzmann distribution with a high-energy Gaussian peak after $0.19\tau_{Debye}(v_0)=1.09$ ps. The initial distribution is given by the dotted line. The electron density was taken to be $n=10^{17}$ cm^{-3} and the initial distribution to comprise a Maxwellian background with a temperature of 3.34 eV together with a Gaussian peak at 33.5 eV.

10 ps. The calculations employed 2×10^5 electrons at a density of $n_e=10^{19}$ cm^{-1}. It is clear that the MD code maintains the Maxwell-Boltzmann distribution, as it should.

It is interesting to test the code against the well-known results obtained by Spitzer [1] under conditions in which his approach is valid. The Spitzer equilibration formula for the rate of equilibration of a two-temperature electron distribution is

$$\frac{dT}{dt}=\frac{T_f-T}{t_{eq}} \tag{14}$$

with

$$t_{eq}=\frac{171\,247}{n_f\ln\Lambda}(T+T_f)^{3/2},$$

where the two groups of particles are denoted ''test'' and ''field,'' with temperatures in eV of T and T_f, respectively, and n_f is the density of the field particles in cm^{-3}.

Figure 3 shows how an initial speed distribution for a group of hot electrons with temperature and density of $T=54.4$ eV and $n=2.0\times10^{14}$ cm^{-3}, respectively, is cooled by field electrons with a temperature and density of $T_f=4$ eV and $n_f=1.0\times10^{16}$ cm^{-3}. The figure shows the initial distribution and that calculated after $\Delta t=198$ ps, corresponding to 13% of t_{eq}. The Coulomb logarithm was taken to be $\ln\Lambda=5$. Cooling of the hot electrons, and corresponding heating of the cold electrons, is clearly observed in the simulation.

The Spitzer formula yields a temperature change for the hot electrons of

$$\Delta T=\Delta t\frac{T_f-T}{t_{eq}}=-6.65\text{ eV}.$$

Since the high-temperature peak is very spread out and non-Maxwellian after $\Delta t=198$ ps it is only a possible estimate of the temperature of the test electrons. By equating the modal energy of the electrons in the high-energy peak to $\frac{3}{2}T_{\text{new}}$, we find $T_{\text{new}}=(48.0\pm1.0)$ eV. Hence the temperature change is found to be $\Delta T=-(6.4\pm1.0)$ eV, in good agreement with the Spitzer result.

Dolinsky [2] has considered the relaxation of a Maxwellian electron energy distribution coexisting with a Gaussian distribution of hot electrons. To describe the temperature and density of the plasma Dolinsky we defined the parameter

$$\frac{k_0}{k_D}=\left(\frac{4\pi\epsilon_0 T}{e^2}\right)^{3/2}\frac{1}{\sqrt{4\pi n}},$$

and chose $k_0/k_D=100$ for his simulations. The formula for the equilibration time Dolinsky uses is

$$\tau_D(v_0)=\frac{(4\pi\epsilon_0)^2m^2v_0^3}{8\pi ne^4\ln\Lambda\left\{\frac{2}{3}\,\text{erf}\left[\sqrt{\frac{3}{2}}\right]-\sqrt{\frac{2}{3\pi}}\exp\left(-\frac{3}{2}\right)\right\}},$$

where v_0 is the root-mean-square velocity of the distribution. If we consider a plasma with an electron density of $n=10^{17}$ cm^{-3}, the condition $k_0/k_D=100$ corresponds to a temperature for the Maxwellian component of 3.34 eV, and the peak of the high-energy Gaussian is at a temperature of 33.5 eV. The value of the Coulomb logarithm used by Dolinsky is not stated, but it is reasonable to assume $\ln\Lambda=5$ for these conditions, giving a relaxation time of $\tau_{Debye}(v_0)=5.73$ ps. Figure 4 shows the initial electron velocity distribution and the distribution calculated for $t=0.19\tau_{Debye}(v_0)$ by Dolinsky and our code. It is clear that our code agrees very well with Dolinsky's result. We note that since the time interval of interest is very short, we could afford to use considerably more particles and more cells for this calculation than for the other calculations in this paper: 1 592 896 particles in 128^3 cells were used to minimize fluctuations in the low-density velocity regime for these calculations. This does not alter the dynamics of the program, since all the parameters are unchanged as well as the number of particles per cell. It does, however, reduce statistical noise and increase the calculation time.

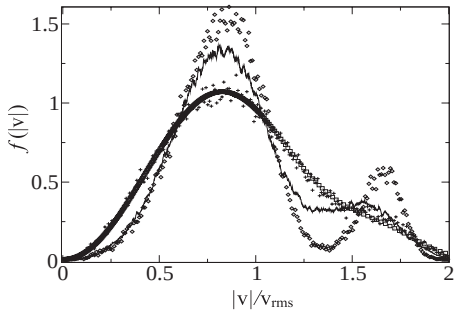

FIG. 5. Comparison of the relaxation of a nonequilibrium distribution of electron energies produced by optical field ionization, as calculated by the Fokker-Planck (squares) and Monte Carlo (diamonds) codes of Refs. [3,4], and by the MD code (solid) described in the present paper. Also shown (crosses) is the distribution calculated by a modified Monte Carlo code in which an averaged Coulomb logarithm was used. For all calculations the electron energy distribution is shown 9.6 ps after the passage of the ionizing laser pulse.

B. Comparison with Monte Carlo and Fokker-Planck calculations in moderately coupled plasmas

We now compare the results of our MD code with recent Fokker-Planck and Monte Carlo calculations by Pert [3] for a far from equilibrium plasma produced by optical field ionization (OFI). Plasmas of this type are of great interest as potential gain media for new types of short-wavelength laser. The comparison presented here shows a discrepancy that might be explained by a breakdown in the assumptions inherent in the use of a Coulomb logarithm.

The initial distribution over electron velocities considered by Pert [3,4] is a plasma created by optical field ionization of helium by a 0.3 ps pulse of circularly polarized light with a peak intensity of 10^{16} W cm^{-2} and a wavelength of 616.4 nm. The optical field ionization formed a plasma with a total electron density of $n=10^{18}$ cm^{-3}, a mean ion charge of 1.2, and an electron energy distribution that comprised two peaks with velocities 5.29×10^{6} m s^{-1} and 1.06×10^{7} m s^{-1}, the lower energy peak containing $\approx$80% of the electrons.

Figure 5 compares the results of our MD calculation with those of Pert at 9.6 ps after the end of the laser pulse [4]. It can be seen that the Fokker-Planck calculation predicts that the energy distribution is essentially equilibrated, whereas the MD and Monte Carlo codes predict that the distribution is still far from equilibrium. The latter two calculations are generally in good agreement with the MD code predicting that the energy distribution is slightly closer to equilibrium than the Monte Carlo calculation. It is interesting to compare these results with the Spitzer equilibration time, Eq. (14). Taking the field particles to be the electrons in the lower-energy peak and the higher-energy electrons to be test particles, we have initial temperatures of $T_f=52.4$ eV and $T=209.5$ eV, and a Coulomb logarithm of approximately $\ln\Lambda=10$. These parameters yield a Spitzer equilibration time of $t_{eq}=73$ ps. Of course, for the case considered here the field particles do not have a Maxwellian distribution, and the proportion of test particles is rather high. However, we would not expect the true equilibration time to be very different from the Spitzer value. As such, 9.6 ps corresponds to $\approx$13% of the equilibration time, and so we would expect the distribution to still be approaching equilibration, which is more consistent with the results of the MD and the Monte Carlo calculations.

The Fokker-Planck calculation employs an average value for the Coulomb logarithm. Figure 5 also shows the results of a Monte Carlo calculation in which the inner cutoff for the Coulomb logarithm has been averaged, rather than being calculated explicitly for each collision [19]. It is seen that the modified Monte Carlo code then agrees very well with the Fokker-Planck calculation which shows clearly how for certain plasma conditions the use of an averaged Coulomb logarithm can give incorrect results. We emphasize that Fokker-Planck codes always assume an average value for the Coulomb logarithm.

C. Application to recombination x-ray lasers

As an example of a calculation that is presently of great interest, but which lies outside the ranges of validity of alternative methods, we consider the relaxation of the electron energy distribution of a mixed plasma formed by the combination of an electrical discharge and optical field ionization. The conditions considered are relevant for a recently proposed scheme for driving soft x-ray lasers in plasma waveguides [20].

Briefly, the proposed scheme operates as follows. It has been demonstrated that discharges through hydrogen-filled capillaries form a parabolic plasma channel able to guide femtosecond laser pulses with peak intensities of 10^{17} W cm^{-2} over lengths of up to 50 mm [21,22]. Very recently a capillary discharge waveguide of this type was used to drive a collisionally excited laser at 41.8 nm in Xe^{8+} ions produced by optical field ionization of Xe atoms doped into the capillary discharge. It has been proposed [20] to extend this idea to recombination lasers in which the relatively cold electrons formed by the discharge rapidly recombine with ions formed by optical field ionization of atoms doped into the plasma channel. Since the rate of three-body electron-ion recombination scales with electron temperature as $T^{-9/2}$ [23], it is crucial for the success of this scheme that the cold discharge electrons are not heated too rapidly by the electrons produced by optical field ionization of the dopant ion. The energy of the electrons produced by OFI may be controlled by the polarization of the ionizing radiation: linear polarization generates relatively cold electrons; circular polarization produces hot electrons. For the proposed laser scheme the primary role of the driving laser is to produce the initial ions which will then recombine with the discharge electrons. The polarization of the driving radiation should then be chosen to reduce the rate of heating of the discharge electrons. The best polarization to use is not obvious. Linearly polarized radiation will produce colder OFI electrons but, using Eq. (14) as a guide, we would expect these to heat the discharge electrons more rapidly than the much hotter electrons generated by circularly polarized radiation. We are presently investigating this problem in detail. Here, we sim-

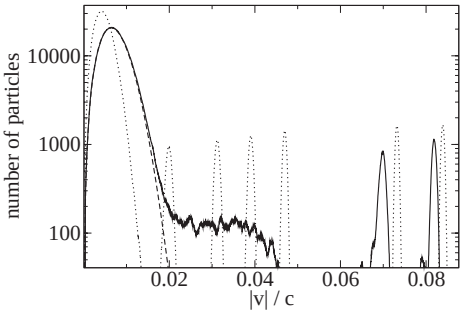

FIG. 6. Calculated relaxation of the electron energy distribution produced by optical field ionization of Ar^{2+} ions in a mixed argon-hydrogen plasma with a temperature of 4.3 eV. The total electron density is 1.06×10^{19} cm^{-3}. The ionizing laser pulse is taken to be circularly polarized with a peak intensity of 1.0×10^{17} W cm^{-2}, a pulse duration of 30 fs, and a wavelength of 566 nm. The initial distribution formed by the discharge and OFI is shown by the dotted curve, and the calculated distribution after 10 ps by the solid line. Also shown is a Maxwellian distribution at 10.5 eV (dashed).

ply provide a sample calculation to illustrate the flexibility of the MD code.

Figure 6 shows the result of a calculation relevant to one example of this scheme: the $4s_{1/2}$-$3p_{3/2}$ transition at 23.2 nm in Ar^{7+}. The capillary discharge is taken to form a plasma with a Maxwellian electron distribution of temperature 4.3 eV and a total electron density of 10^{19} cm^{-3}. The initial Ar density is taken to be 10^{17} cm^{-3}. Under these conditions, the argon is ionized by the discharge to Ar^{2+}. The precursor to the lasant ion Ar^{8+} is produced by optical field ionization with a circularly polarized pulse of radiation of wavelength 566 nm and a peak intensity of 1.0×10^{17} W cm^{-2}, thereby generating six classes of hot electrons with energies ranging from 100 eV to 1800 eV. Figure 6 shows the calculated relaxation of the initial electron energy distribution formed by the discharge and optical field ionization. Note that the abscissa has a logarithmic scale in order to show the OFI peaks more clearly. It is seen that within 10 ps after the formation of the optical field ionization the four lowest-energy OFI peaks have merged into the tail of the distribution of discharge electrons. In contrast, the highest two OFI classes remain as distinct peaks and show only a slight cooling on this time scale. If one were to use the Spitzer equilibration times [Eq. (14)] for these peaks, keeping in mind that this formula is not strictly valid for these parameters, the lowest-energy peak would have an equilibration time $t_{eq}\approx2$ ps and for the highest-energy peak $t_{eq}\approx130$ ps, which at least qualitatively agrees with the observed relaxation of the peaks. Of key importance to the proposed recombination laser scheme is the heating of the discharge electrons at 4.3 eV by the hot OFI electrons. Figure 6 also shows a Maxwellian distribution at 10.5 eV which fits the bulk of the low-energy part of the energy distribution very well. We conclude, therefore, that the presence of the electrons generated by OFI of Ar heats the cold discharge electrons by ≈6 eV in 10 ps. Whether this heating is sufficiently slow to allow rapid recombination with the Ar^{8+} ions will be the subject of future work. In the meantime we emphasize that the conditions considered here fall outside the range of validity of the assumptions made by Spitzer: a plasma which is far from equilibrium; a relatively high proportion of test particles; and a small number of particles in the Debye sphere ($N_{Debye}<10$). For this last reason, any approach that incorporates a Coulomb logarithm is likely to produce inaccurate results.

IV. CONCLUSION

In summary, we have described a molecular-dynamic code for calculating the relaxation of an arbitrary electron energy distribution in a plasma. To our knowledge, this is the first time that the MD approach has been used to treat this problem.

In Sec. III A we showed that the MD code is in agreement with earlier work, in their ranges of validity. The MD approach treats the problem at a more fundamental level, and therefore can be expected to have a wider range of validity than alternative approaches. As such it is an extremely flexible technique for investigating the relaxation of the electron energy distribution in plasmas, as well as providing a reliable benchmark against which to test faster, more specialized codes.

In order to illustrate the flexibility of the MD code we have considered two examples lying outside the range of validity of alternative methods. In Sec. III B we showed that for a plasma produced by optical field ionization a Fokker-Planck calculation can yield inaccurate results, and in Sec. III C we considered a moderately coupled plasma ($N_{Debye}\approx10$). Understanding energy relaxation in plasmas of this type is important for understanding the operation of new types of short-wavelength lasers based upon optical field ionization.

ACKNOWLEDGMENTS

The authors would like to acknowledge helpful discussions on this problem with Professor S. J. Rose and Professor G. J. Pert, and would like to thank Professor Pert for sending the results of his modified Monte Carlo code. S.M.H. is grateful to the Royal Society and N.D. to the Rhodes Trust.

[1] L. Spitzer, *Physics of Fully Ionized Gases* (Interscience Publishers, New York, 1962).
[2] A. Dolinsky, Phys. Fluids **8**, 3 (1965).
[3] G.J. Pert, J. Phys. B **32**, 27 (1999).
[4] G.J. Pert, J. Phys. B **34**, 881 (2001).
[5] G.J. Pert, Phys. Rev. E **51**, 4778 (1995).
[6] D.O. Gericke *et al.*, Phys. Rev. E **65**, 036418 (2002).
[7] J.P. Hansen and I.R. McDonald, Phys. Lett. **97A**, 42 (1983).
[8] U. Reimann and C. Toepffer, Laser Part. Beams **8**, 4771 (1990).
[9] M.S. Murillo, Phys. Rev. Lett. **87**, 115003 (2001).
[10] G. Zwicknagel *et al.*, Contrib. Plasma Phys. **33**, 395 (1993).

[11] R. Hockney and J. Eastwood, *Computer Simulations Using Particles* (McGraw-Hill, New York, 1981).
[12] Z. Donko and G.J. Kalman, Phys. Rev. E **63**, 061504 (2001).
[13] W.H. Press *et al.*, *Numerical Recipes in C* (Cambridge University Press, Cambridge, 1992).
[14] C.K. Birdsall and A.B. Langdon, *Plasma Physics via Computer Simulation* (IOP, New York, 1995).
[15] H.J. Kull, *Computer Simulation von Plasmen, Skriptum zur Vorlesung* (RWTH, Aachen, 2001).
[16] F. John, *Partial Differential Equations* (Springer, Berlin, 1978).
[17] W. Ames, *Numerical Methods for Partial Differential Equations* (Academic Press, New York, 1992).
[18] F. Scheck, *Mechanik* (Springer, Berlin, 1996).
[19] G.J. Pert (private communication).
[20] D.J. Spence *et al.*, J. Opt. Soc. Am. B **20**, 138 (2003).
[21] A. Butler *et al.*, Phys. Rev. Lett. **89**, 185003 (2002).
[22] D.J. Spence *et al.*, J. Phys. B **34**, 4103 (2001).
[23] G.J. Pert, J. Phys. B **23**, 619 (1990).